ZESZYTY NAUKOWE POLITECHNIKI ŚLĄSKIEJ 1987

Seria: ENERGETYKA z. 98 Nr kol. 1022

Tadeusz CHMIELNIAK
Andrzej WITKOWSKI

AN ANALYTICAL METHOD FOR THE DETERMINATION OF AERODYNAMIC PERFORMANCE OF AXIAL COMPRESSOR STAGES

Summary. The new method of analysis of aerodynamic losses in axial flow compressor stage, and particularly annulus wall boundary layer losses has been elaborated. The problem has been solved both in the theoretical and experimental way. The method relies on interpretation of results obtained by comparing the distribution of useful work and blades work along blade hight, obtained succesively from the analysis of inviscid and real flow structure. As a result of this, the profile friction, annulus wall friction and the secondary flow losses were identified. This work gives a good basis for determining the calculated method of simulation of aerodynamic characteristics of compressor stages.

SYMBOLS

C_f - Skin friction coefficient

$\bar{F}_b$ - blade force vector

$f = \frac{F_b}{A_k}$ - blade force per unit cross sectional area of stream tube

H - shape parameter

i - static enthalpy

L - work

ΔL - loss work

$\dot{m}$ - mass flow

m - meridional direction

r - radius coordinate

t_c - tip clearance

t - blade spacing of cascade

t_ϑ - profile thickeness in tangential direction

ϑ - number of impeller blades

β - relative flow angle from meridional plane

δ - angle between meridional streamline and axis of rotation, boundary layer thickness

δ^* - boundary layer displacement thickness

δ^{**} - boundary layer momentum thickness

δ_f - force deficit thickennes

Φ - angular coordinate

ρ - density

τ - wall shear stress

ν - kinematic viscosity

$(\ )_e$ - at the edge of boundary layer

$(\ )_1, (\ )_2$ - upstream and downstream of blade row

$(\bar{\ })$ - mean values

$(\ )_h$, $(\ )_o$ - at the hub and at the outer wall

$(\hat{\ })$ - quantities calculated as a result of solving the axial symmetrical flow problem after taking into consideration blockage factor.

1. Introduction

The general purpose of this study was to obtain and verify the information necessary to develop a practical digital computer program which could be used to describe aerodynamic characteristic of single stage of axial compressor of arbitrary geometry at design and off design flows and speed. The problem has been solved by the theoretical and experimental investigations of the flow structure and impeller aerodynamic loadings in the model axial flow compressor stage [1].
In theoretical part the relations between character of velocity and pressure distribution along the hub and the casing wall, and development of annulus wall boundary layers on the one hand, and magnitude of loss taking place in the flow on the other hand have been established.
The problem has been solved taking into consideration the simplified so called quasireal flow model in which to make the analysis easier, the flow has been devided into two regimes: the main stream flow where the effects of viscosity are negligible and where only the profile losses exist and two areas at the hub and the outer wall where an annulus boundary layer is created. The main flow problem has been solved utilising the quasi-threedimensional flow model in which two problems succesively has been analysed:

1) the problem of the axial symmetrical flow,
2) the problem of the blade cascade flow on choice axialsymmetrical surfaces of flow.

The axial symmetrical problem was solved by Streamline Curvature Method after circumferentially averaged equation of motion for steady and non-viscous flow.
As a result of solving the axially symmetric flow equations, boundary layer growth along the hub and outer wall and losses occuring in this zones have been determined. A discussion of auxiliary relationships required for predicting the boundary layer and accuracy of different methods of solving has been made. The new equation for the relationship between the components of the blade defect force has been specified. To obtain additional information about the flow through the axial flow compressor stage and to make the verification of proposed computing methods possible, a test stand for investigation of aerodynamic loading of impeller blades and for determining of the flow structure in the chosen cross section for the selected coefficient of flow has been created. The essential part of this work is identification of the quantities of the characteristic parameters of annulus wall boundary layers in function of aerodynamic load, of the stage, and position of measured cross section.
The analysis of the results of experimental investigation of the flow structure was the basis for a new method of establishing the elaboration of aerodynamic losses in the blade row, and particularly the losses occuring close to the annulus walls. That method made possible in turn, to elaborate the conception of simulation of axial compressor stage performance in an analitycal way.

2. Theory

2.1. Mainstream flow

The axialsymmetrical problem was solved by Streamline Curvature Method after circumferentially averaged equation of motion for steady and non-viscous flow. The general equation of axisymmetric motion for a fluid flowing relative to a turbomachine rotor in cylindrical rotating coordinates r, ϑ, z is [2], [3]:

$$W \frac{\partial W}{\partial q} + P \cdot W^2 + Q \cdot W + R = 0 \qquad (1)$$

The procedure for utilising equation (1) to obtain a solution on a prescribed stream surface is to estimate the function $P(q)$, $Q(q)$, $R(q)$ [2], [3] so that equation of continuity:

$$\dot{m} = Z \int_0^q \left[q \cdot W \cdot \cos\beta \cos(\delta - \gamma) \frac{2\pi r}{Z} - t_\vartheta \right] dq \qquad (2)$$

be satisfied. The flow calculation in model compressor stage [1] has been performed in 32 quasiorthogonals and [11] streamlines (Fig. 1). The computer program STO PZDW [4] has been applied.

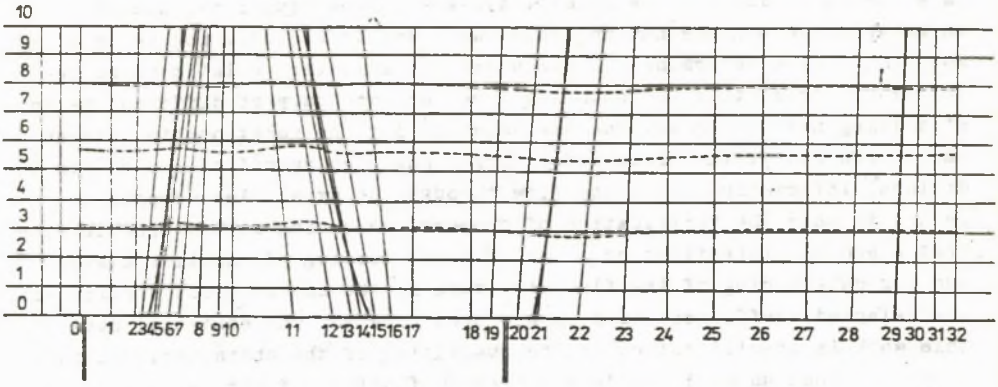

Fig. 1. Quasiorthogonal grid in the meridional crossection of the compressor stage

Rys. 1. Siatka quasiortogonalnych w przekroju merydionalnym stopnia sprężarki

2.2. End wall boundary layer theory

2.2.1. Basic equations

In order to calculate the growth of the annular boundary layers the authors made use of a set of two momentum integral equations which enable the calculation of the growth of the momentum thickness in meridional and tangential direction [5], [6]:

$$\frac{d}{dm}\left(\bar{W}_m^2 \delta_m^{**}\right) + H\delta_m^{**}\bar{W}_m \frac{d\bar{W}_m}{dm} = \frac{d}{dm}\left(\frac{\bar{W}^2}{2}\,\delta_{fm}\right) + \frac{\bar{\tau}_{om}}{\rho} \tag{3}$$

$$\frac{d}{dm}\left(W_m W_\vartheta \delta^{**}\right) + H\delta_m^{**}\bar{W}_m \frac{d\bar{W}_\vartheta}{dm} = \frac{d}{dm}\left(\frac{\bar{W}^2}{2}\,\delta_{f_\vartheta}\right) + \frac{\bar{\tau}_{o\vartheta}}{\rho} \tag{4}$$

The velocities $\bar{W}_m(m)$ and $\bar{W}_\vartheta(m)$ on the outer edge of the boundary layer, in successive sections of the flow system, are found from the analysis of the axisymmetric flow. After determining the initial walues δ_1^{**} and H_1 in the inlet to the blade - ring, seven unknowns: τ_m, τ_ϑ, f_m, f_ϑ, δ_{m2}, $\delta_{\vartheta 2}$ as well as H_2 are left. Thus it is necessary to find some new complementary equations [6].

2.2.2. Methods of solution

The equations (3) and (4) together with the complementary equations which are most often determined by way of experiment, form a set of closed equations the solution of which enables the calculation of all boundary layer parameters. Various forms of empirical, complementary equations which are used in most methods, raise doubts as regards the range of their importance [5], [7], [8]. The authors carried out the analysis concerning the influence of the forms of complementary equations as well as experimental quantities appearing in them on the results of calculations concerning the growth of boundary layers.
Three methods were made use of in the analysis:

Method 1

By considering the overall changes in axial momentum across a blade row, both for the boundary layer and for the mainstream flow Stratford [9] derived a momentum integral equation for the axial growth of the boundary layer. Stratford assumed that the body force is normal to the blades and remains constant in the boundary layer. With the above assumptions we obtain from equation (3) the momentum integral equation for the meridional direction:

$$\frac{d}{dm}\left(\bar{W}^2\delta_m^{**}\right) + H \cdot \delta_m^{**} \cdot \bar{W}_m \frac{d\bar{W}_m}{dm} = \frac{\tau_m}{\rho} \tag{5}$$

The empirical formula for the value of shear stresses was made use of as complementary equation in the considered method. This formula was determined for a two-dimensional flow on a flat plate by a stream running at an angle β to the axis X:

$$\tau_m = \tau_w \cdot \cos\beta = 0{,}086 \cdot \rho \cdot W_m^{9/5} \cdot (\sec\beta)^{4/5} \cdot \nu^{1/5} \cdot \delta^{**1/5} \tag{6}$$

The next dependence closing the system of equations is empirical correlation of shape factor H with the axial gradient of axial velocity and the momentum thickness Reynolds number $Re_{\delta^{**}} = W_m \cdot \delta^{**}/\nu$:

$$H = 1{,}67 - 0{,}09 \cdot \log Re_{\delta^{**}} - 0{,}11 \frac{\delta^{**}}{W_m}\frac{dW_m}{dm} \cdot 10^3 + $$
$$+ 0{,}015 \cdot \left(10^3 \frac{\delta^{**}}{W_m} \cdot \frac{dW_m}{dm}\right) \tag{7}$$

Method 2

It is the method worked out by Mellor and Wood [5]. As basic equations the dependencies (3) and (4) are used here. They are complemented by the equations determining the variation of constituent axial and wall shear stresses:
for the flow of a hub impeller:

$$\frac{\tau_m}{\rho} = C_f/2 \left[C_m^2 + (U - C_\vartheta)^2\right]^{1/2} \cdot C_m \tag{8}$$

$$\frac{\tau_\vartheta}{\rho} = C_f/2 \left[C_m^2 + (U - C_\vartheta)^2\right]^{1/2} \cdot (U - C_\vartheta) \tag{9}$$

for the flow of an outer wall

$$\frac{\tau_m}{\rho} = C_f/2 \left[C_m^2 + (W_\vartheta - U)^2\right]^{1/2} \cdot C_m \tag{10}$$

$$\frac{\tau_\vartheta}{\rho} = C_f/2 \left[C_m^2 + (W_\vartheta - U)^2\right]^{1/2} \cdot (W_\vartheta - U) \tag{11}$$

In order to obtain a complete set of equations further relations were determined between the momentum thickness δ^{**}_ϑ, δ^{**}_m, and between axial and tangential components of blade force defects δ_{fm} and $\delta_{f\vartheta}$.
The first equation was obtained [5] as a result of treating blade to blade flow as the superposition of primary flow taking place on the axial - symmetrical stream surfaces as well as of secondary flows:

$$W_{\vartheta 2}(\delta^{**}_{\vartheta 2} - \delta^{**}_{m2}) = K \cdot t_c \left[t/l \cdot C_e(C_{\vartheta 2} - C_{\vartheta 1})\right]^{1/2} \cdot \mathrm{sign}(C_{\vartheta 2} - C_{\vartheta 1}) \tag{12}$$

The significant disadvantage of this equation is the fact that it determines only the conditions in the outlet section of the impeller. In this paper the drawback of the method was coped with by assuming the linear variation of the expression $(\delta^{**}_{\vartheta 2} - \delta^{**}_{m2})$ between the inlet and outlet section of the blade. At the same time $\delta^{**}_{\vartheta 1} = 0$. The closing equation determines the relationship between the axial and tangential components of blade force, which was derived under the assumption that the direction of that force is no subject to change in the area of the boundary layer:

$$\overline{W}_m \frac{d}{dm}\left(\frac{\overline{W}_e^2}{2}\delta_{fm}\right) + (1 - \varepsilon)\overline{W}_\vartheta \frac{d}{dm}\left(\frac{\overline{W}_e^2}{2}\delta_{f\vartheta}\right) = 0 \tag{13}$$

Method 3

The significant difference of the method in comparison with method 2 consists in the replacement of the equation determining the relationship between the blade defect forces δ_{fm} and $\delta_{f\vartheta}$ in the form of (13) by an additional equation which takes into consideration the influence of skin friction and secondary stresses, which was introduced in paper [6]. This relationship which additionally takes into account apparent secondary stress $\rho \cdot \overline{W'_m \cdot W'_r}$ in the direction of the axle m and $\rho \cdot \overline{W'_\vartheta \cdot W'_r}$ in the direction of the axle r has the form [6]:

$$\frac{\bar{W}_e^2}{2}\delta'_{fm} + tg\beta\frac{\bar{W}_e^2}{2}\delta_{f\vartheta} = \frac{\bar{W}_e^2}{4}(\bar{\tau}_f + \bar{\tau}_s) \cdot h - (\bar{\tau}_m + \bar{\tau}_\vartheta \cdot tg\beta)\Delta m \qquad (14)$$

The dependence (14) testifies to the physically recognized relationship between the distribution of blade forces in the boundary layer, and the quantity of shear stress loss and secondary losses.

3. The loss analysis in annulus wall boundary layer

3.1. General remarks

The mathematical model of losses was worked out in virtue of integral parameters of the boundary layer. The determination of the reduction of the stream of mass as well as the reduction of the circumferential forces in boundary areas at the hub and at the casing wall, is of fundamental importance.

3.2. The reduction of the stream of mass

Denoting by $\hat{W}_m$ meridional velocity determined form the calculations of the mainstream and by W_m velocity appearing in the flow with regard to skin friction, one obtained as a result an equation which takes into account casing wall displacement by the value of displacement ghickness at the hub δ^*_h and at the casing wall δ^*_o:

$$\frac{\dot{m}}{2\pi\rho} = \int_{r_h}^{r_o} r\,\hat{W}_m\,dr - (W_{me}\,\delta^* \cdot r)_o - (W_{me}\,\delta^* \cdot r)_h \qquad (15)$$

3.3. Work and energy consideration

The equation determining actual rotor blade forces can be shown in the way analogous to the equation of real stream of mass:

$$\int_{r_h}^{r_o} r \cdot U \cdot f_\vartheta \cdot dr = \int_{r_h}^{r_o} r \cdot U \cdot f_\vartheta \cdot dr - r_o U_o \int_{r_o-\delta_o}^{\delta_o} (\hat{f}_\vartheta - f_\vartheta) dr -$$

$$- r_h \cdot U_h \cdot \int_{r_h}^{r_h+\delta_h} (\hat{f}_\vartheta - f_\vartheta)_h \cdot dr \tag{16}$$

Takind into consideration the equation of force deficit thickness in boundary areas [5] and the dependence determining the composite profile of blade forces:

$$f_\vartheta(r) = \tilde{f}_\vartheta(r) + \hat{f}_\vartheta(r) - f_{\vartheta_e} \tag{17}$$

we rearrange the equation (16) to the form:

$$\int_{r_p}^{r_o} r \cdot U \cdot f_\vartheta \cdot dr = \int_{r_h}^{r_o} r \cdot U \cdot \hat{f}_\vartheta \cdot dr - r_o \cdot U_o \cdot \frac{W_o^2}{2} \delta_{f\vartheta o} -$$

$$- r_h \cdot U_h \cdot \rho \frac{W_h^2}{2} \delta_{f\vartheta h} \tag{18}$$

3.4. Circumferential components of blade forces

The distribution of the components of circumferential velocities has direct influence on the value of cirucmferential components of blade forces as well as on the value of work transmitted by the blade ring and finally on the losses appearing in the areas of boundary layers. The tangential blade force is calculated from the dependence:

$$f_{\vartheta,k} = \frac{F_{b,k}}{A_k} = C_{m,k} \cdot \rho \cdot \Delta C_{\vartheta,k} \tag{19}$$

3.5. The analysis of losses in the axial compressor impeller

A new method of identification of boundary losses was applied. It is based on the analysis of distribution of useful work along the height of the blade as well as on the work transmitted by the blades of the impeller, as a result of the appropriate working out of the results of flow traversing [6], [10]. The real work transmitted by the blades of the rotor to the compressed factor can be represented by the dependance:

$$L_t = \int_{r_h}^{r_\rho} \rho \cdot Wm \cdot \Delta i^* \cdot r \cdot dr = \int_{rh}^{r_\rho} U \cdot f_\vartheta \cdot r \cdot dr + \Delta L_t =$$

$$= \int_{r_p}^{r_\rho} r \cdot U \cdot f_\vartheta \cdot dr - \sum_{p,o} r \cdot U \cdot \frac{\overline{W}^2}{2} \delta_{f\vartheta} + \Delta L_f \qquad (20)$$

Analysing the equation (20) with making use of the dependence (15), as well as (17) and (18) we come to the formulas which calculate the losses in the flow system of the blade ring.

The losses of useful work:

- the loss of useful work in boundary areas as a result of the reduction of the rate of flow:

$$\Delta L_{u,\Delta\dot{m}} = 2\pi \left[\int_{r_h}^{r_\rho} \rho \cdot \Delta \hat{i}_s^* \cdot W_m \cdot r \cdot dr - \int_{r_h+\delta_h^*}^{r_o-\delta_o} \rho \cdot \Delta \hat{i}_s^* \cdot \hat{W}_m \cdot r \cdot dr \right] \qquad (21)$$

- the loss of useful work as a result of the reduction of pressure in the areas of boundary layers:

$$\Delta L_{u,\Delta p} = 2\pi \left[\int_{r_h+\delta_n^*}^{r_\rho-\delta_o^*} \rho \Delta \hat{i}_s^* \cdot \hat{W}_m \cdot r \cdot dr - \int_{r_h}^{r_o} \rho \cdot \Delta i_s^* \cdot W_m \cdot r \cdot dr \right] \qquad (22)$$

The sum of losses of useful work is at the same time the sum of all boundary losses appearing in the flow through the blade ring:

$$\Delta L_b = \Delta L_{u,\Delta\dot{m}} + \Delta L_{u,\Delta p} = 2\pi \left[\int_{r_h}^{r_o} \rho \cdot \Delta \hat{i}_s^* \cdot W_m \cdot r \cdot dr - \right.$$

$$\left. - \int_{r_h}^{r_o} \rho \cdot \Delta i_s^* W_m \cdot r \cdot dr \right] \qquad (23)$$

Making use of the common coefficient of friction losses and of secondary flows ($\bar{\zeta}_{f,s} = \bar{\zeta}_f + \bar{\zeta}_s$) appearing in the equation (14) it is furthermore possible to isolate friction losses and secondary flow losses from boundary ones:

$$\Delta L_{t,w} = \dot{m} \cdot \bar{\zeta}_{fs} \cdot \overline{W}_1^2/2 \qquad (24)$$

3.5.1. The losses of blade work

The loss of blade work as a result of the reduction of the rate of flow

$$\Delta L_{f,\Delta\dot{m}} = 2\pi\left[\int_{r_b}^{r_o} \hat{f}_\psi \cdot Z \cdot r \cdot dr - \int_{r_h+\delta_h^*}^{r_o,\delta_o^*} \hat{f}_\psi \cdot U \cdot r \cdot dr\right] \tag{25}$$

- the loss of blade work as a result of the reduction of tangential blade forces

$$\Delta L_{f,f_\psi} = 2\pi\left[\int_{r_h+\delta_h^*}^{r_o-\delta_o^*} \hat{f}_\psi \cdot U \cdot r \cdot dr - \int_{r_h}^{r_o} f_\psi \cdot U \cdot r \cdot dr\right] \tag{26}$$

- total blade loss

$$\Delta L_f = \int_{r_h}^{r_o} \hat{f}_\psi \cdot U \cdot r \cdot dr + \Delta L_{fr} - \int_{r_h}^{r_o} \hat{f}_\psi \cdot U \cdot r \cdot dr -$$

$$- \sum_{h,o} r \cdot U \cdot W^2/2\, \delta f_\psi + \Delta L_{fr} \tag{27}$$

Generalized losses

The loss of isentropic flow

$$\Delta L_s = \int_{r_h}^{r_o} \hat{f}_\psi \cdot U \cdot r \cdot dr + \Delta L_{fr} - \int_{r_h}^{r_o} \rho\, \hat{W}_m \cdot \Delta \hat{i}_s^* \cdot r \cdot dr \tag{28}$$

- Profile loss

$$\Delta L_p = \int_{r_h}^{r_o} \hat{f}_\psi \cdot U \cdot r \cdot dr + \Delta L_{fr} - \int_{r_h}^{r_o} \rho \cdot \hat{W}_m \cdot \Delta \hat{i}_s^* \cdot r \cdot dr \tag{29}$$

The complete loss of compressor stage is the sum of boundary and profile losses:

$$\omega u_{T,st} = \Delta L_b + \Delta L_p = \int_{r_h}^{r_o} f_\varphi \cdot U \cdot r \cdot dr + \Delta L_{fr} -$$

$$- \int_{r_h}^{r_o} \rho \cdot \Delta i_s^* \cdot W_m \cdot r \cdot dr \qquad (30)$$

4. Test stand

The results of theoretical predictions are compared with experimental investigation which has been performed on the test stand for determining the flow structure in axial compressor stage (Fig. 2). The flow system of the examined compressor stage consists of an impeller row with eighteenth blades the design being free vortex, discharge back stator vans and the outflow curvilinear diffuser. A detailed description of the research stand is in the authors paper [2]. Flow traverses were made before and behind rotor at three flow coefficients (C_m/U_T = 0,317, 0,37, and 0,4475). In the main stream a five hole probe was used but for the boundary layer flows a three tube Conrad type probe was needed to make accurate measurements close to the walls.

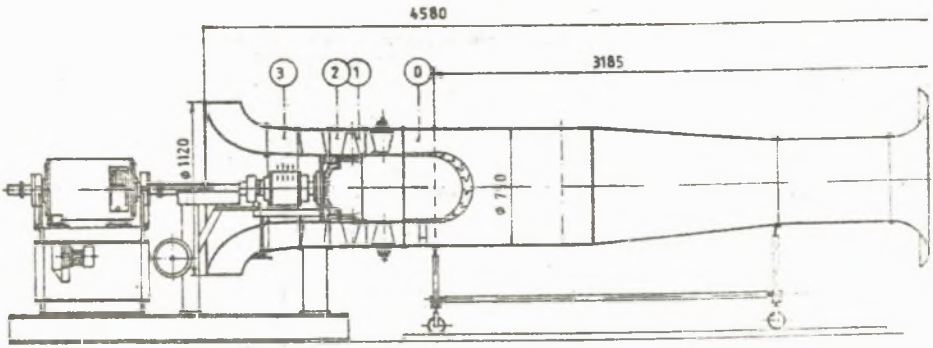

Fig. 2. Test stand
Rys. 2. Stanowisko badawcze

5. Discussion of results

5.1. Mainstream velocity profiles

Figures 3, 4 and 5 show the theoretical and experimental results for the axial velocity distribution at the upstream and downstream of the rotor. The influence of annulus boundary layer growth on theoretically de-

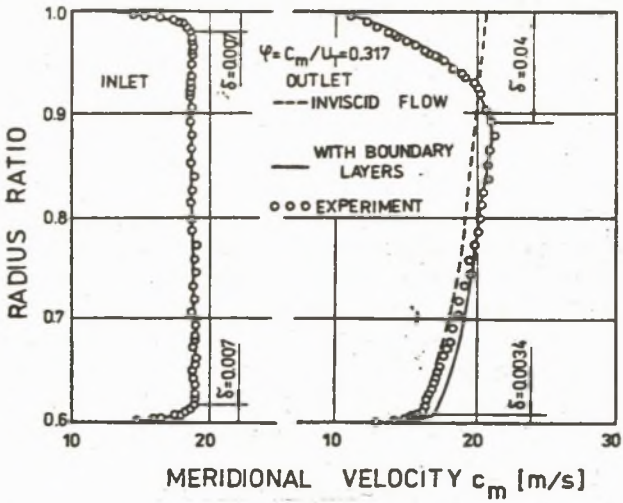

Fig. 3. Velocity profiles upstream and downstream of blade impeller at $\varphi_T = 0{,}317$

Rys. 3. Profile prędkości w przekroju wlotowym i wylotowym łopatek wirnika przy $\varphi_T = 0{,}317$

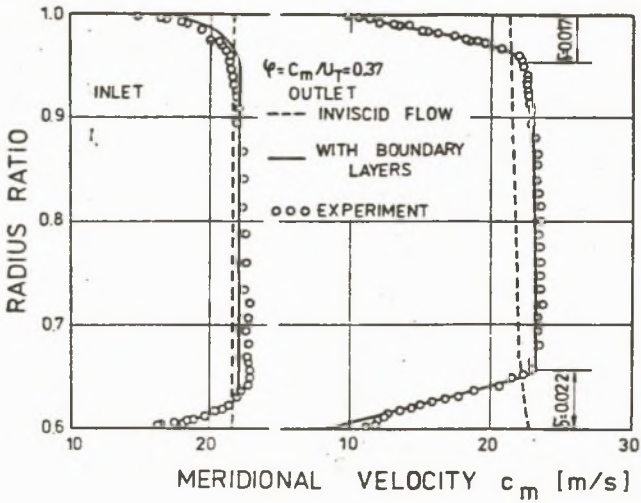

Fig. 4. Velocities profiles upstream and downstream of blade impeller at $\varphi_T = 0{,}37$

Rys. 4. Profile prędkości w przekroju wlotowym i wylotowym łopatek wirnika przy $\varphi_T = 0{,}37$

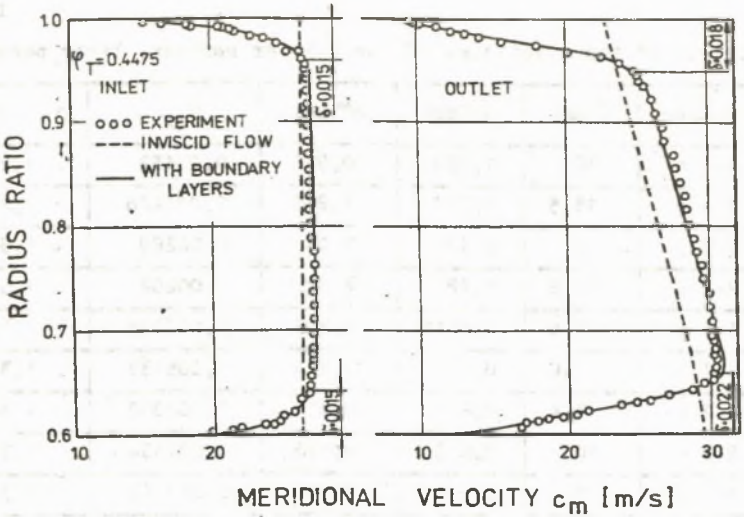

Fig. 5. Velocities profiles upstream and downstream of blade impeller at t φ_T = 0,4475

Rys. 5. Profile prędkości w przekroju wlotowym i wylotowym łopatek wirnika przy φ_T = 0,4475

fined velocity distributions in the main flow has been considered by applying blockage factor. The resulting velocity free stream profiles have been matched with boundary layer velocity profiles calculated by mean for r Coles formula [11]. The same tendences in theoretically and experimentally set in meridional velocity profiles in the downstream of the impeller should be stressed. The meridional velocity along the radius may increase, remain constant or decrease depending on the flow coefficient. These changes in axial velocity are very important when considering the boundary layers.

6. Identification of the annulus boundary layer parameters

The velocity distributions served to calculate the measuring values of thickness of boundary layers. The aim of the analysis was to determine the influence of working point and the location of measuring section on the formation of velocity profiles in boundary areas at the hub and at the casing wall as well as on the quantities of the annular boundary layer parameters: δ, δ^*, δ^{**}_m, δ^{**}_ϑ, $\delta_{f\vartheta}$, δ_{fm}, H.

The results of the analysis are set together in table 1.

Table 1

The comparison of the quantities of the annular boundary layer parameters

φ_T	Section	δ[mm]	δ^*[mm]	δ^{**}[mm]	C_{fx}	H
0,37	1-1 p	16	1,229	0,946	0,00432	1,273
	1-1 o	13,5	1,557	1,201	0,004228	1,2984
	2-2 p	26	4,18	3,04	0,00289	1,375
	2-2 o	14,5	3,28	2,08	0,00292	1,5749
0,317	1-1 p	7,0	0,6619	0,506	0,005698	1,300
	1-1 o	7,0	0,82	0,624	0,005137	1,314
	2-2 p	3,4	0,6	0,412	0,004802	1,3420
	2-2 o	10	7,673	5,488	0,002534	1,398
0,4475	1-1 p	15	2,046	1,538	0,005588	1,33
	1-1 o	15	1,7	1,316	0,00398	1,2958
	2-2 p	22	4,966	3,187	0,001989	1,558
	2-2 o	18	5,517	2,899	0,001262	1,9185

7. The growth of the annular boundary layers

The results of the concerning the growth of the annular boundary layers were obtained using three methods discussed at point 2, at the three points of aerodynamic characteristic of the model compressor ring [1], [3] (φ_T = 0,317, 0,37, 0,4475) [6]. They were compared with the integral parameters of the boundary layer determined by way of experiment [3] in inlet and outlet section of the rotor. The results obtained with the use of method 3 point to the possibility of obtaining an arbitrary accuracy of calculations by an appropriate selection of clearance leakage ratios K as well as the coefficients of friction losses and secondary flows $\bar{\zeta}_{f,s}$ [6]. The exemplary diagram concerning the growth of the annular boundary layers at the nominal point φ_T = 0,37 was shown in figure 6.

8. Calculation of losses

The balance of losses appearing in the rotor row of axial compressor was carried out in virtue of the equation derived before for three flow coefficients. A new method of calculating boundary losses was applied here. It is based on the analysis concerning the distribution of useful

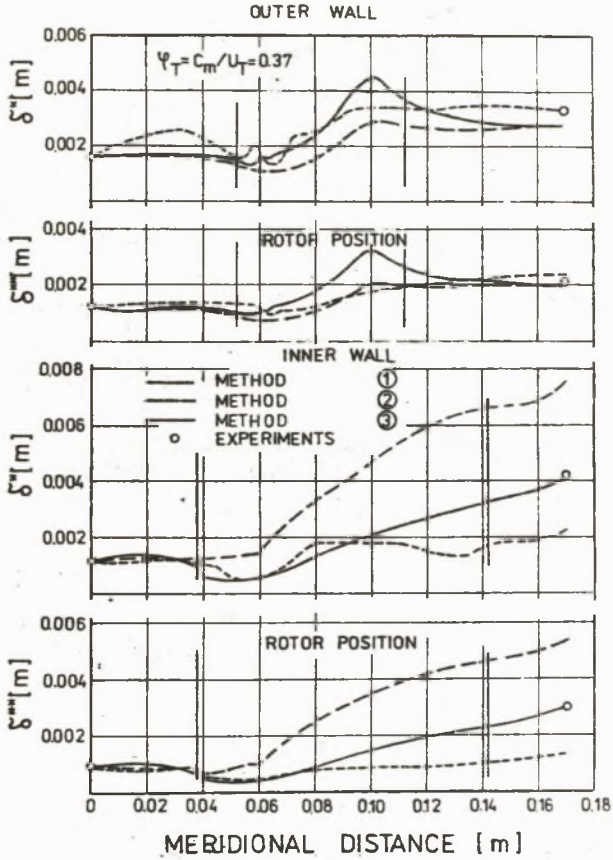

Fig. 6. Rotor boundary layer growth at φ_T = 0,37

Rys. 6. Narastanie pierścieniowych warstw przyściennych w kole wirnikowym przy φ_T = 0,37

work as well as the work transmitted by the blades of the rotor, obtained as a result of an appropriate working out of the results of flow traversing. These results are shown in figures 7, 8, 9, 10, 11, 12. The loss of work because of friction against axialsymmetrical limiting surfaces is calculated making use of the relations:

- in the boundary area at the hub

$$\Delta L_{th} = \frac{C_f}{2}\left\{W_m^2 + (U - C_{\varphi})^2\right\}^{1/2} (U - C_{\varphi})\, 2\pi \cdot r \cdot \Delta m \cdot U \qquad (31)$$

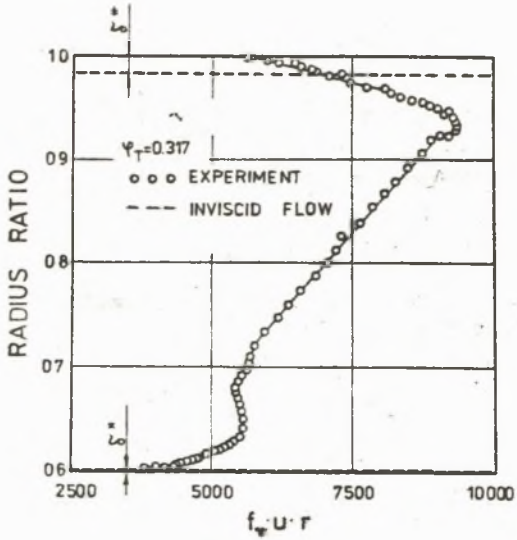

Fig. 7. Distribution of the useful work at φ_T = 0,317
Rys. 7. Rozkład pracy użytecznej przy φ_T = 0,317

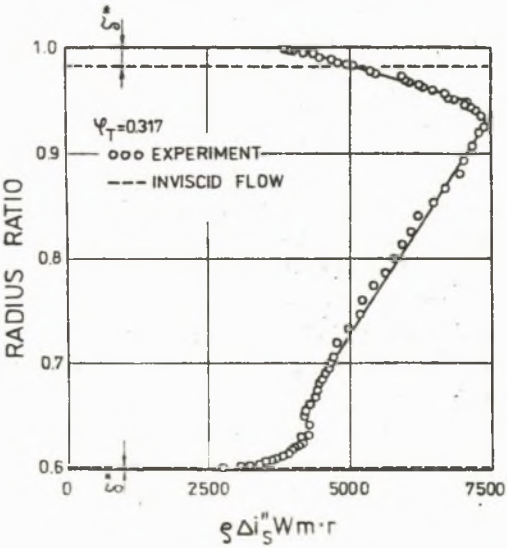

Fig. 8. Distribution of the blade work at φ_T = 0,317
Rys. 8. Rozkład pracy łopatkowej przy φ_T = 0,317

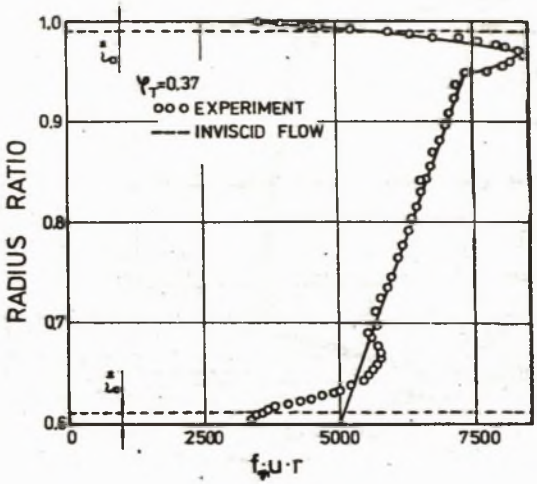

Fig. 9. Distribution of the useful work at φ_T = 0,37
Rys. 9. Rozkład pracy użytecznej przy φ_T = 0,37

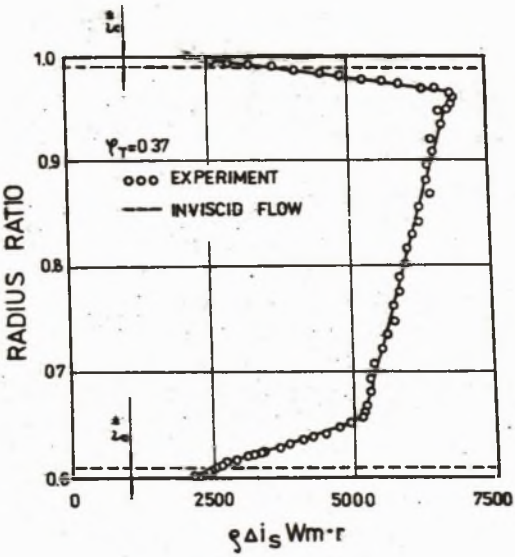

Fig. 10. Distribution of the blade work at φ_T = 0,37
Rys. 10. Rozkład pracy łopatkowej przy φ_T = 0,37

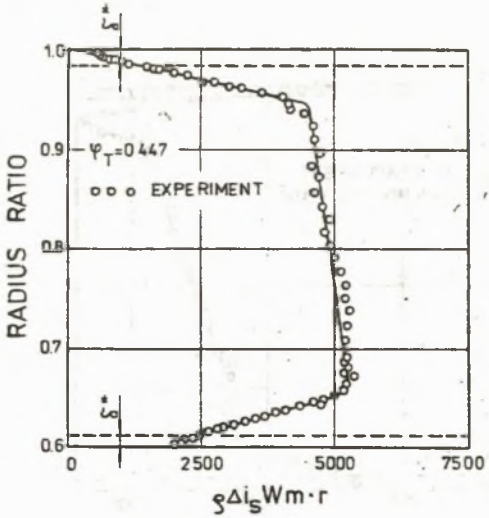

Fig. 11. Distribution of the useful work at φ_T = 0,4475
Rys. 11. Rozkład pracy użytecznej przy φ_T = 0,4475

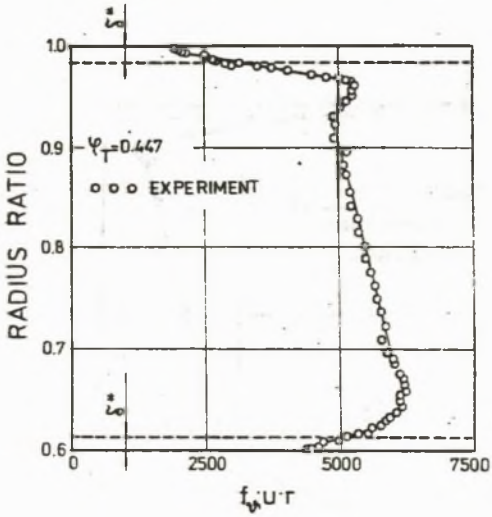

Fig. 12. Distribution of the blade work at φ_T = 0,4475
Rys. 12. Rozkład pracy łopatkowej przy φ_T = 0,4475

- in the boundary area at the casing wall

$$\Delta L_{to} = \frac{C_f}{2}\left\{W_m^2 + (U - W_\vartheta)^2\right\}^{1/2} (U - W_\vartheta)\, 2\pi r \Delta m U \tag{32}$$

and is set together in table 2.

Table 2

The list of the value of the shear stress work

Kind of surface	$\varphi_{T\ min} = 0{,}317$	$\varphi_{T\ nom} = 0{,}37$	$\varphi_{T\ max} = 0{,}4475$
Hub	19,56	9,307	13,663
Casing well	5,07	3,96	10,32
Sum	24,56	13,267	29,983

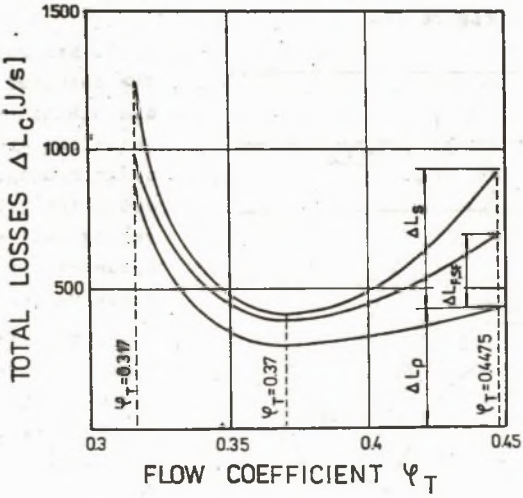

Fig. 13. Profile and boundary losses in the function of coefficient of flow

Rys. 13. Straty profilowe i brzegowe w wieńcu wirnikowym w funkcji wskaźnika wydajności

The calculated profile and boundary losses appearing in the flow system of the rotor ring are shown in figure 13. The losses of friction and of secondary flows determined by the equation (24) were also isolated here. The analysed losses balance satisfactory total losses of work in the compressor ring only at design point of work (φ_T = 0,37). However at

the off design points of the characteristic there is a considerable range of losses which were not isolated in this paper. Mainly the losses resulting from clearance leakage belong to them.

9. The proposed method of predicting axial compressor stage performance characteristics by way of calculation

The results concerning the analysis of the structure of flow presented in this paper suggest a four-grade procedure of calculating aerodynamic characteristic of the compressor ring by way of calculation:

1. In the first order the axial - symmetrical problem is solved without taking into consideration the influence of viscosity, making use only of the characteristics of the cascades termined along the height of the blade row, beginning from the hub and ending at the casing wall. It leads as a consequence to "smooth" distribution of the axial and circumferential components of velocity, which makes it possible to calculate the theoretical characteristics of the stage for the axial-symmetrical flow $\psi_{t-a} = f(\varphi_T)$ shown in figure 14.

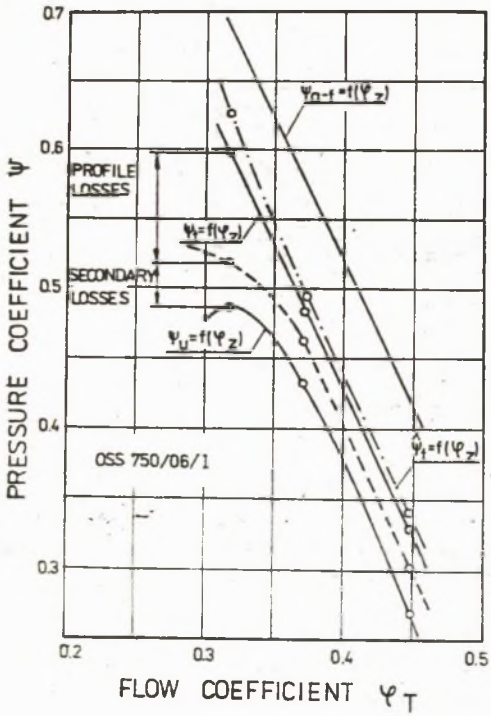

2. Nex making use of the obtained velocity distributions one calculates the growth of annular boundary layers along the hub and the casing wall and as a consequence - the values of blocking the main flow.

3. Then it is necessary to repeat the calculations of the axialsymmetrical flow making use of the data determined at point 2. The profiles of velocity obtained by

Fig. 14. Consecutive phase of rotor performance characteristics on an analytical way

Rys. 14. Kolejne fazy wyznaczania charakterystyki aerodynamicznej wieńca wirnikowego na drodze obliczeniowej

this means are termed in this paper the profiles of the main flow and are determined like other quantities by the index ($\wedge$). The theoretical pressure coefficient calculated from that were determined in figure 14 as Ψ_T.

4. The distributions of velocities of the main flow agreed with the profiles of velocity in the annular areas of the boundary layers, in the blade-to-blade spaces, create in turn the possibility of calculating real work transmitted by the blade ring. These work is represented in figure 14 by the pressure coefficient Ψ_T. The calculation of friction losses, the profile as well as the boundary ones, leads to the calculation, of the real characteristic of the impeller $\Psi_u = f(\varphi_T)$ (fig. 14). The extension of the presented analytical scheme to the whole compressor stage composing the example from the rotor ring and the stator blade row does not create greater substantial problems.

10. Conclusions

Analysing the structure of flow in the axial compressor impeller the authors isolated profile losses, boundary losses taking into consideration the losses appearing in the boundary areas as well as the secondary flow losses. According to figure 13 the above mentioned losses balance satisfactorily the complete losses in the rotor blades only at the design point of the work (φ_T = 0,37). However at the off design flows of the characteristic there is a considerable range of losses which were not isolated in this work. Mainly the losses connected with clearance leakage belong to them.

REFERENCES

[1] Witkowski A.: "Arrangement for Testing of the Flow Structure in Axial Compressor Stage" (in Polish) ZN Pol. Śl. Energetyka z. 72 1979, pp. 199-210.

[2] Witkowski A. "Flow Analysis in Axial - Flow Compressor Impeller with Meridional Stream Acceleration. Proc. of the Fourth Conference on Fluid Machinery Budapest 1972, pp. 1515-1541.

[3] Witkowski A.: "Influence of Aerodynamic Load on the Shape of Velocity Profiles in the Axial Flow Compressor Stage. Proceedings of the Seventh Conference on Fluid Machinery. Akademiai Kiado, Budapest 1983, pp. 948-956.

[4] Witkowski A.: "Program Algol 1900". Concerning the Calculations a Axial Symmetrical Flow in Axial-Compressor Stage (unpublished paper). Gliwice 1982.

[5] Mellor G.L. and Wood G.M.: "An Axial Compressor End Wall Boundary Layer Theory. Trans. ASME, Journal of Basic Engineering, Juni 1971, pp. 300-317.

[6] Witkowski A.: "The Theoretical and Experimental Analysis of the Flow Structure in Axial Compressor Stage" (in Polish) ZN Pol. Śl. Energetyka, z. 93, Gliwice 1986, pp. 1-158.

[7] Balsa T.F. and Mellor G.L. "The Simulation of Axial Compressor Performance Using an Annulus Wall Boundary Layer Theory". Trans. ASME, J. Eng. for Power, July 1975, pp. 305-318.

[8] Cyrus V.: "The Blade Force Defect in the Calculation Method of the End Wall Boundary Layer in Axial Compressor". Strojirenstvi, vol. 28 No 9, 1978, pp. 515-520.

[9] Stratford B.S.: "The Use of Boundary Layer Techniques to Calculate the Blockage from the Annulus Boundary Layer, in a Compressor". ASME Raport No 67-WA/GT-7, pp. 1-8.

[10] Chmielniak T. and Szymczyk K.: "The Simulation of Dissipative Boundary Effects in Blade Rings of Turbomachines" (in Polish). ZN Pol. Poznań 1982, pp. 65-69.

[11] Coles D.: "The Law of the Wall in the Turbulent Boundary Layer", J. Fluid Mech., I, 1956, pp. 191.

Recenzent: Doc. dr inż. Jan Radwański

Wpłynęło do Redakcji w marcu 1987

OBLICZENIOWA METODA WYZNACZANIA CHARAKTERYSTYKI AERODYNAMICZNEJ OSIOWEGO STOPNIA SPRĘŻAJĄCEGO

S t r e s z c z e n i e

Opracowano nową metodę analizy strat aerodynamicznych występujących w osiowym stopniu sprężającym w szczególności strat generowanych w obszarach pierścieniowych warstw przyściennych. Zagadnienie zostało rozwiązane na drodze wzajemnie się uzupełniającej analizy teoretycznej i doświadczalnej.

W części teoretycznej określono związki występujące pomiędzy charakterem rozkładu prędkości i ciśnień wzdłuż ścianek ograniczających przepływ, a narastaniem warstw przyściennych z jednej strony oraz wielkością strat występujących w przepływie z drugiej strony. Zagadnienie rozwiązano rozpatrując uproszczony tak nazwany "quasirzeczywisty" model przepływu, w którym dla ułatwienia analizy wyodrębniono charakterystyczne obszary: obszar przepływu głównego, w którym pomija się wpływ tarcia przyściennego, a uwzględnia jedynie straty profilowe oraz dwa obszary przy piaście i osłonie zewnętrznej, gdzie tworzy się pierścieniowa warstwa przyścienna.

Dla uzyskania uzupełniających informacji dotyczących przepływu przez osiowe stopnie sprężające oraz dla umożliwienia weryfikacji proponowanych metod obliczeniowych, skonstruowano stanowisko do badań obciążeń aerodynamicznych wirujących wieńców łopatkowych oraz struktury przepływu w wybranych przekrojach kontrolnych stopnia, zarówno w układzie względnym jak i bezwzględnym, w obliczeniowym i pozaobliczeniowych punktach pracy. Odpowiednie opracowanie wyników sondowania przepływu umożliwiło opracowanie nowej metody identyfikacji strat brzegowych na podstawie analizy roz-

kładu wzdłuż wysokości łopatki pracy użytecznej oraz pracy przekazywanej przez łopatki koła wirnikowego. W rezultacie wyodrębnione zostały straty profilowe, straty tarcia występujące w obszarach przyściennych oraz straty przepływów wtórnych.

Uzyskane wyniki stwarzają dobrą podstawę opracowania metody umożliwiającej wyznaczenie charakterystyk aerodynamicznych osiowych stopni sprężających na drodze obliczeniowej.

РАСЧЁТНЫЙ МЕТОД ОПРЕДЕЛЕНИЯ АЭРОДИНАМИЧЕСКОЙ ХАРАКТЕРИСТИКИ ОСЕВОЙ КОМПРЕССОРНОЙ СТУПЕНИ

Р е з ю м е

Разработан новый метод анализа аэродинамических потерь в осевой компрессорной ступени, в особенности потерь выступающих в области кольцевого пограничного слоя. Задача была разрешена теоретическим и экспериментальным путём. Метод основывается на интерпретации результатов сравнения полезной и лопаточной работ, полученных по соответствующей обработке результатов зондирования реального течения по радиусу лопаточного венца колеса. Этот метод сделал возможным, в свою очередь, разработку концепции предусмотрения аэродинамических характеристик компрессорных ступеней расчётным методом.